Original scientific paper

A RIGOROUS MODEL FOR FREQUENCY-DEPENDENT FINGERPAD FRICTION UNDER ELECTROADHESION

Fabian Forsbach, Markus Heß

Department of System Dynamics and Friction Physics, TU Berlin, Germany

Abstract. *In the electroadhesive frictional contact of a sliding fingerpad on a touchscreen, friction is enhanced by an induced electroadhesive force. This force is dominated by the frequency-dependent impedance behavior of the relevant electrical layers. However, many existing models are only valid at frequency extremes and use very simplified contact mechanical approaches. In the present paper, a RC impedance model is adopted to characterize the behavior in the relevant range of frequencies of the AC excitation voltage. It serves as an extension to the macroscopic model for electrovibration recently developed by the authors, which is based on several well-founded approaches from contact mechanics. The predictions of the extended model are compared to recent experimental results and the most influential electrical and mechanical parameters are identified and discussed. Finally, the time responses to different wave forms of the excitation voltage are presented.*

Key words: *Friction, Adhesion, Electrovibration, Surface Haptics, Tactile Display*

1. INTRODUCTION

Electrovibration is a powerful technology of surface haptics that enables effective tactile feedback on touch screen surfaces of smartphones, tablets, navigation systems and similar devices of consumer electronics. It uses electrostatic attraction to enhance sliding friction between a fingerpad and touch surface. This can be done by applying an AC voltage to the conductive layer of the screen, which causes polarization of the fingerpad, resulting in an electroadhesive contribution to the normal contact force that increases the frictional force. The latter is controlled by changing the amplitude, shape and frequency of the voltage to create a variety of different tactile effects [1, 2].

Although the magnification of the perceived frictional force caused by an alternating voltage, was known far earlier, before Grimnes [3], named this effect "electrovibration",

it is still not fully understood today. One major problem represents the complex coupling between contact mechanics and electrodynamics, which is why highly simplifying assumptions are often made in theoretical modeling. Even without considering electrostatic interactions, understanding the tribological behavior of human skin including its effect on tactile perception is a challenging task because of the layered structure and non-linear visco-elastic material behavior of the skin. In addition, the skin surface of the fingerpad has a very specific topography and its ridges are far away from being smooth. They are punctuated by a variety of concave shaped sweat pores which allow to lubricate the skin and hence change its tribological properties [4, 5]. The induced electrostatic interaction between the fingerpad and conductive layer of the screen in the state of full slip further increases the difficulty in finding a suitable model. In the last decade, intensive research has been carried out on the study of the electrodynamics of contact, both experimentally and theoretically, and several interesting models have emerged [6, 7, 8]. However, experiments are often carried out under restrictive contact mechanical conditions, such as a fixed apparent contact area, although it is obvious that the contact area of the real, electroadhesive frictional contact depends on both the normal force and the applied voltage. If the corresponding measurement results serve as the basis for theoretical modeling, effects like the reduction of the (apparent and ridge) contact area during transition from stick to slip caused by an increasing tangential force cannot be considered. Moreover, the mechanical part of the contact is often represented only in the simplest way via a combination of spring and damper [9].

Recently, the authors proposed a new macroscopic model for electrovibration that is based on several well-founded approaches from contact mechanics [10]. The model provides plausible results for all contact mechanical quantities, particularly, it adequately predicts the friction force and the friction coefficient over the entire range of relevant voltages and applied normal forces, which is supported by a comparison with experimental results. However, in the electrodynamic part of the model, the outer layer of skin, the interfacial air gap and the coating of the conductive layer of the screen are assumed to be purely capacitive. Therefore, the applicability of the model is limited to high-frequency excitations.

In the present paper, the electrodynamic part is improved by considering the resistive properties of all three components to represent the frequency dependence of the frictional force. For this purpose, the RC impedance model proposed by Shultz et al. [8] is adopted.

The manuscript is structured as follows: At the beginning of Chapter 2, we first briefly summarize the main approaches of the model recently proposed by the authors to map electrovibration. Subsequently, the improvement of its electrodynamic part is explained in detail which allows to study the frequency dependence of the frictional force. Chapter 3 is addressed to the relevant electrical and mechanical parameters for the coating of the touchscreen, the stratum corneum, the interfacial air gap and the ridge contact area as a function of the applied normal force used in our simulations. Since no experimental study provides a complete set of measured relevant parameters, they had to be taken from various works. Chapter 4 contains the results emerging from the simulations with the new electromechanical model. The influence of numerous parameters on the electrostatic contribution to the frictional force as a function of frequency is analyzed and compared with known experimental data. The time response is studied for both a pure sinusoidal and a square-wave excitation. Some conclusive remarks in Chapter 5 close the manuscript.

2. MACROSCOPIC MODEL FOR ELECTROADHESION

In a recent work the authors propose a macroscopic model for the frictional contact between a fingerpad and an AC voltage supplied coated touch surface in a state of full slip (Fig. 1). In contrast to highly simplified models, it is based on sound contact mechanics approaches, which are briefly summarized below. For a detailed description of the model, the reader is referred to the original paper [10].

Pressure-controlled friction is assumed, i.e., the frictional force obeys the generalized Amontons-Coulomb law [11], which includes an additional contribution to the normal contact force to account for electroadhesive interaction:

$$F_T = \mu_0(F_N + F_{el}) = \mu_0(F_N + \sigma_{el}A_R) \,. \tag{1}$$

It should be noted that Eq. (1) emerges as a limiting case of the adhesive tangential contact in a Coulomb-Dugdale approximation as well [12]. μ_0 and F_N denote the friction coefficient and the applied normal force, respectively. σ_{el} represents the electrodynamic contribution to the normal contact force per unit area which can be expressed in terms of the air gap thickness d_a and voltage U_a

$$\sigma_{el} = \frac{\varepsilon_0 \varepsilon_{r,a} U_a^2}{2 d_a^2}. \tag{2}$$

A_R is the ridge contact area in a state of full slip, which is significantly smaller than the ridge contact area $A_{R,0}$ under pure normal loading. Supported by experiments [13] and FE simulations [10], the decrease of the ridge contact area during the transition from stick to slip can be described by
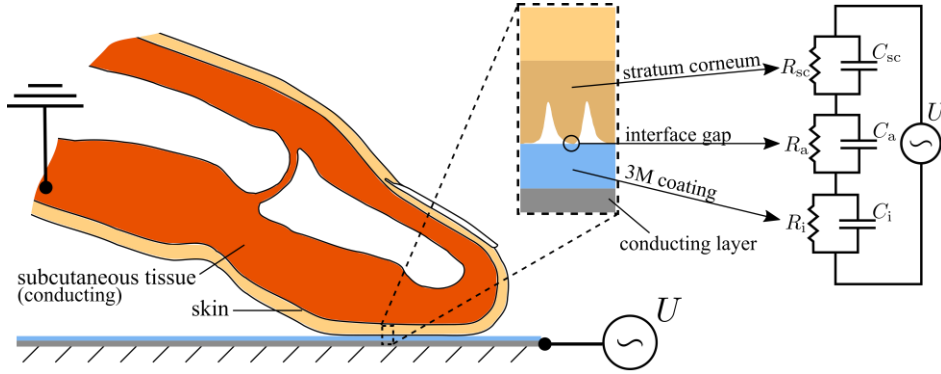
Fig. 1 Electroadhesive frictional contact with the relevant layers of the finger-touchscreen interface and their representation in the RC impedance model

$$A_R(F_T) = A_{R,0} - \frac{c_2}{A_{R,0}} F_T^2. \tag{3}$$

The empirical parameter c_2 must be determined by experiments, FE simulations or similar. The ridge contact area under pure normal loading, but taking into account adhesion, must be determined from the following equation that results from Shull's compliance method

$$F_{\mathrm{N}}\left(A_{\mathrm{R},0}\right) = \alpha^{-1/m} A_{\mathrm{R},0}^{1/m} - \sqrt{\frac{2wn^2}{n-m}\beta^{1/n}\alpha^{-1/m}A_{\mathrm{R},0}^{1+1/m-1/n}}, \qquad (4)$$

where α, β, m and n are parameters of non-adhesive powerlaw-relationships between ridge contact area $A_{\mathrm{R},0}$ and normal force F_1 as well as indentation depth δ_1, namely

$$A_{\mathrm{R},0}(F_1) = \alpha F_1^m, \qquad (5)$$

$$A_{\mathrm{R},0}(\delta_1) = \beta \delta_1^n, \qquad (6)$$

and w denotes the work of electroadhesion per unit area (see [10] for details). In the present paper the parameters in Eqs. (5) and (6) are taken from experimental data (see Section 3.4 and Table 1 for details). According to Heß and Popov [14], the work of electroadhesion per unit area can be calculated by

$$w = \int_{d_{\mathrm{a}}}^{\infty} \sigma_{\mathrm{el}}(\tilde{d}_{\mathrm{a}})\mathrm{d}\tilde{d}_{\mathrm{a}}. \qquad (7)$$

By using Eqs. (1) to (7), the authors calculated the friction coefficient and friction force which both agree well with experimental measured data over the entire range of relevant voltages and applied normal forces [10]. However, since the outer layer of skin, the interfacial air gap and the coating of the conductive layer of the screen are assumed to be purely capacitive, the applicability of the model is restricted to the high-frequency regime. Here, we improve the electrodynamic part of the model by mapping the impedance of each electrical layer as a resistor in parallel with a capacitor (Fig. 1).

Now, suppose a sinusoidal excitation voltage

$$U(t) = U_0 \sin(\Omega t). \qquad (8)$$

The impedance of each layer is then given by

$$Z_x = \frac{R_x}{1 + i R_x C_x \Omega}, \ x \in \{\mathrm{i,a,sc}\}, \qquad (9)$$

with the capacitances C_x and resistances R_x of the respective layer. For the RC circuit depicted in Fig. 1, the amplitude $U_{\mathrm{a},0}$ of the voltage across the interfacial air gap,

$$U_{\mathrm{a}}(t) = U_{\mathrm{a},0} \sin(\Omega t + \varphi), \qquad (10)$$

relates to the amplitude of the excitation U_0 as

$$\frac{U_{\mathrm{a},0}}{U_0} = \left| \frac{Z_{\mathrm{a}}}{Z_{\mathrm{i}} + Z_{\mathrm{a}} + Z_{\mathrm{sc}}} \right|. \qquad (11)$$

With Eq. (9), this equation can be written as

$$\frac{U_{\mathrm{a},0}}{U_0} = \frac{\dfrac{R_{\mathrm{a}}}{\sqrt{1 + \tau_{\mathrm{a}}^2 \Omega^2}}}{\sqrt{\left(\dfrac{R_{\mathrm{a}}}{1 + \tau_{\mathrm{a}}^2 \Omega^2} + \dfrac{R_{\mathrm{i}}}{1 + \tau_{\mathrm{i}}^2 \Omega^2} + \dfrac{R_{\mathrm{sc}}}{1 + \tau_{\mathrm{sc}}^2 \Omega^2}\right)^2 + \left(\dfrac{R_{\mathrm{a}}\tau_{\mathrm{a}}\Omega}{1 + \tau_{\mathrm{i}}^2 \Omega^2} + \dfrac{R_{\mathrm{i}}\tau_{\mathrm{i}}\Omega}{1 + \tau_{\mathrm{i}}^2 \Omega^2} + \dfrac{R_{\mathrm{sc}}\tau_{\mathrm{sc}}\Omega}{1 + \tau_{\mathrm{sc}}^2 \Omega^2}\right)^2}}, \qquad (12)$$

where $\tau_i = R_i C_i$, $\tau_a = R_a C_a$ and $\tau_{sc} = R_{sc} C_{sc}$. The phase angle of the gap voltage $U_a(t)$ is given by

$$\varphi = \arctan \left[\frac{R_{sc} \dfrac{(\tau_{sc} - \tau_a)\Omega}{1 + \tau_{sc}^2 \Omega^2} + R_i \dfrac{(\tau_i - \tau_a)\Omega}{1 + \tau_i^2 \Omega^2}}{R_a + R_{sc} \dfrac{1 + \tau_a \tau_{sc} \Omega^2}{1 + \tau_{sc}^2 \Omega^2} + R_i \dfrac{1 + \tau_a \tau_i \Omega^2}{1 + \tau_i^2 \Omega^2}} \right]. \tag{13}$$

In the limiting case of very small frequencies, the electrical circuit behaves purely resistive, yielding

$$\lim_{\Omega \to 0} \left(\frac{U_{a,0}}{U_0} \right) = \frac{R_a}{R_i + R_a + R_{sc}}, \tag{14}$$

whereas for high frequencies the behavior is purely capacitive, yielding

$$\lim_{\Omega \to \infty} \left(\frac{U_{a,0}}{U_0} \right) = \frac{C_i C_{sc}}{C_i C_a + C_a C_{sc} + C_i C_{sc}}. \tag{15}$$

The latter equation leads to the original model of [10].

3. ELECTROMECHANICAL PARAMETERS

The electrical and mechanical parameters used for the model are listed in **Table 1**. To the authors knowledge, there is unfortunately no experimental investigation where the complete set of relevant parameters is measured.

The capacitances for the three different layers can be determined *via*

$$C_x = \frac{\varepsilon_0 \varepsilon_{r,x} A_R}{d_x}, \ x \in \{i, a, sc\}, \tag{16}$$

where ε_0 is the permittivity of free space, $\varepsilon_{r,x}$ is the relative permittivity of the respective layer and d_x is the thickness of the layer.
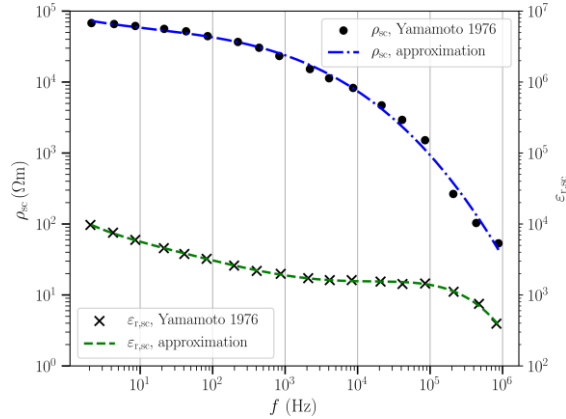
Fig. 2 Resistivity ρ_{sc} and relative permittivity $\varepsilon_{r,sc}$ of stratum corneum taken from [17]

3.1. 3M coating

The commonly used 3M coating of the touchscreen is 1µm thick and the relative permittivity $\varepsilon_{r,i}$ is usually given with 3.9 [2]. Due to the high resistivity of silica (SiO$_2$), the coating is often described as an insulator [6, 7]. However, in [15], a resistive behavior is measured for low frequencies which may be the result of imperfections in the 3M coating. An adequate approximation of the impedance measured in [15] in the relevant frequency range can be achieved by the circuit in Fig. 1, a capacitator with the properties of the silica layer parallel to a resistor with $R_i=0.2M\Omega$.

3.2. Stratum corneum

The resistance of the stratum corneum is determined *via*

$$R_{sc} = \frac{\rho_{sc} d_{sc}}{A_R},$$
(17)

with the resistivity and thickness of stratum corneum ρ_{sc} and d_{sc}, respectively. The thickness varies in the range of 200-450 µm [16]. Its electrical properties are highly frequency-dependent. The resistivity ρ_{sc} and relative permittivity $\varepsilon_{r,sc}$ in the relevant range of frequencies was measured by [17]. Fig. 2 shows the experimental data as well as the fits

$$\rho_{sc} = 10^{-0.023z^3+0.0795z^3-0.2133z^2+4.9229} \ \Omega m$$
(18)

and

$$\varepsilon_{r,sc} = 10^{-0.00286z^5+0.03564z^4-0.15785z^3+0.33963z^2-0.6235z+4.1598},$$
(19)

where $z=\log_{10}(f / 1Hz)$. These fits were used in the model to account for the frequency-dependent behavior.

Table 1 Parameters for the model of sliding friction

Symbol	Parameter name	Value and unit
μ_0	Friction coefficient	0.3
F_N	Applied normal force	$F_N = 0.5$ N
$\varepsilon_{r,i}$	Relative permittivity of 3M coating	3.9
$\varepsilon_{r,a}$	Relative permittivity of the interfacial gap (air)	1
ε_0	Permittivity of free space	$8.854 \cdot 10^{-12}$ As/Vm
d_i	Thickness of the 3M Coating	1 µm
d_a	Thickness of the interfacial gap	3.5 µm
d_{sc}	Thickness of stratum corneum	350 µm
R_a	Resistance of the interfacial gap	$1 \cdot 10^6 \ \Omega$
R_i	Resistance of the 3M Coating	$2 \cdot 10^5 \ \Omega$
$m, n,$	Parameters of power-law expressions for ridge	$m=0.52, n=1.41,$
α, β	contact area	$\alpha=54.4mm^2/N^m, \beta=32.0$ mm^{2-n}
c_2	Empirical parameter for area reduction	$c_2 = 5000$ mm^4/N^2

3.3. Interfacial gap

The properties of the interfacial air gap are a subject of current research. However, recent studies [8, 9] indicate an equivalent gap thickness d_a of 1-5µm between the finger pad ridges and the comparatively smooth display surface. This is further supported by topography measurements of the microstructures on the ridge [18]. The experimentally observed resistance of the interfacial gap is mainly a constriction resistance of the rough contact. The charges can only pass the interfacial gap at the microcontacts or at fluid filled spots and can thus not flow freely. This gap resistance is therefore highly dependent on the interface properties such as the amount of sweat produced by the sweat ducts or contamination. To the authors knowledge there is no direct measurements of the gap resistance, but in [8] a value of 7 MΩ is determined indirectly.

3.4. Ridge contact area

The ridge contact area A_R is a further highly subject dependent quantity. The parameters for the power-law relations of the non-adhesive ridge contact area (Eqs. (5) and (6)) in Table 1 are taken from [19]. Thus, at a normal force of 0.5N non-adhesive ridge contact area is measured to approximately 37mm². However, this value can vary significantly depending on the finger size and its angle to the contacting surface. In the following section, the influence of the ridge contact area is investigated by keeping the exponents m and n in the power-law relations in Eqs. (5) and (6) constant but scaling the parameters α and β accordingly. The parameter c_2 controlling the area reduction due to the tangential loading is taken from [10].

4. FREQUENCY DEPENDENCE OF ELECTROADHESION

In this section, the model prediction of the electroadhesive contribution to the normal force F_{el} is investigated and compared to experimental data by [6]. Furthermore, the influences of the uncertain equivalent thickness and resistance of the interfacial gap as well as the subject dependent thickness of the stratum corneum and ridge contact area are investigated.

Fig. 3 shows the model predictions of the average inferred electroadhesive force in terms of the excitation frequency and the experimental data found by [6] for different subjects. The black curves correspond to the parameters in Table 1. Furthermore, a variation in the experimentally found ranges is shown for the parameters listed above.

In all cases, the model predictions show the same characteristics: For low frequencies, the electrical circuit behaves mainly resistive and the voltage across the interfacial gap approaches the limit in Eq. (14). The inferred electroadhesive force is proportional to the square of that voltage, $F_{el} \propto U_a^2$ (see Eq. (2)), and therefore also approaches a limit value. Similarly, for frequencies higher than 2000 Hz the circuit is mainly capacitive (see Eq. (15)) and the electroadhesive force approaches another, larger limit. In agreement with the experimental data, the forces increase by up to 80% from 100 Hz to 10000 Hz.

For decreasing thickness of the stratum corneum and increasing ridge contact area (on the upper left and right of Fig. 3, respectively), the electroadhesive force increases approximately linearly in the whole frequency spectrum. However, compared to the variations in the thickness of the stratum corneum, small differences in the ridge contact area have far greater influence on the force. In [20], using another, much simpler modeling approach, the wide-

spread experimental results were explained by the variability in the thickness of the stratum corneum. With the mechanically and electrically much more comprehensive model presented in this paper, this result cannot be confirmed.
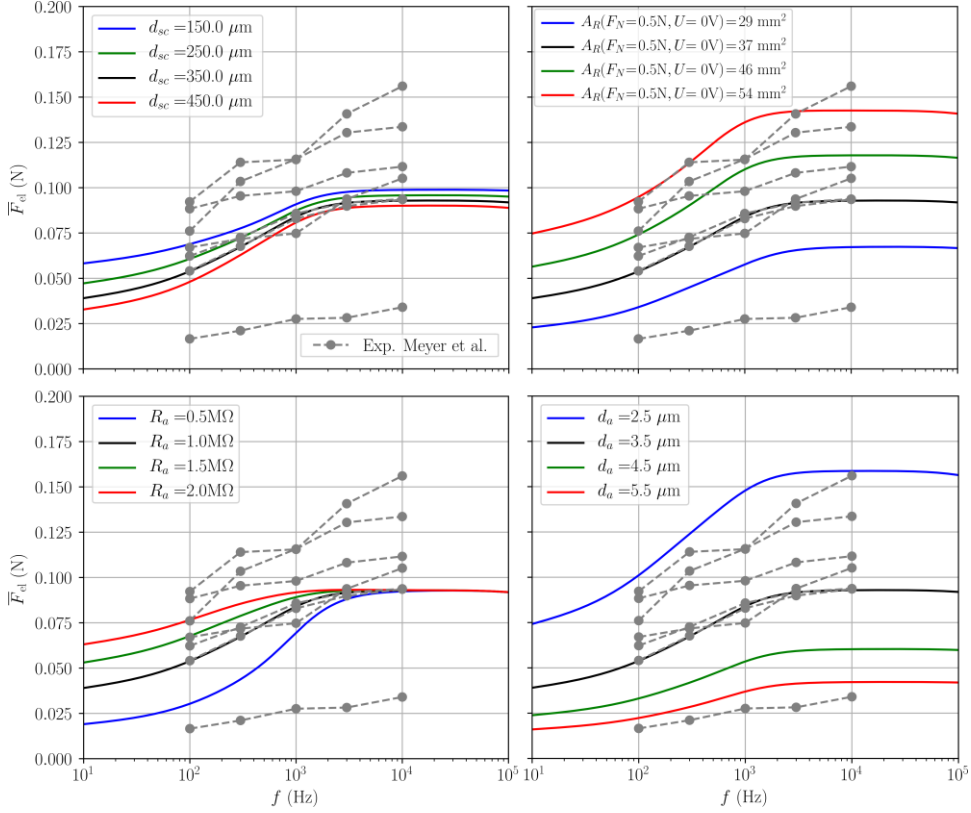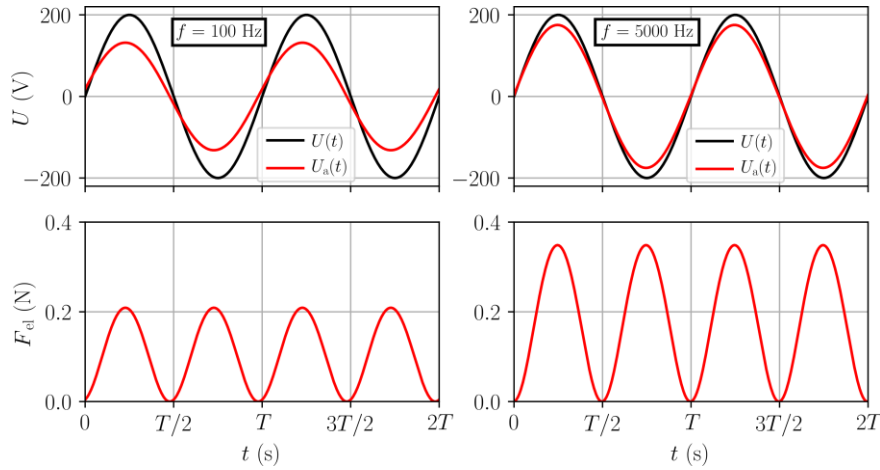

Fig. 3 Inferred electroadhesive force F_{el} in terms of Excitation frequency f for an excitation voltage amplitude of $U_0 = 140$V and an external force of F_N=0.5N predicted by the proposed model and, in grey, experimentally found by [6]

The influence of the interfacial gap parameters is shown on the lower left and right of Fig. 3. If the resistance of the interfacial gap is increased, the force in the resistance-dominated low frequency range is increased as well. For the proposed model, values in the range of 1-2MΩ appear appropriate. This range is significantly lower than the value calculated in [15] (7MΩ). However, the interface resistance is expected to vary extensively depending on multiple interface and environmental parameters as described in Section 3.3. The equivalent interfacial gap thickness influences the whole frequency range significantly (see lower right of Fig. 3). The range of 2-5µm appears appropriate and is, as described in Section 3.3, in agreement with the values found in the literature. In light of Eq. (12) and $C_a \ll C_{sc}$ as well as $C_a \ll C_i$, the electroadhesive force is roughly proportional to $(d_a)^{-2}$ and, thus, increases rapidly for small interfacial gap thicknesses.

The experimental data points for the different subjects in Fig. 3 vary extensively: Some show convergence for high frequencies, while other do not (yet) converge and in addition there is a significant quantitative scatter. The reason for this is unclear and requires further experimental investigation. Particularly, measurements of (ridge) contact area and skin hydration level of the different subjects are of interest. Unfortunately, to the authors' knowledge, this is the only experimental investigation of the frequency dependence. Thus, while adequate agreement with some individual subjects is possible by fitting of the parameters in the discussed ranges (see for example the black curve in Fig. 3), the model should be validated with a more complete data set of a future experimental study. However, the parameter variations discussed above offer some possible explanations for the observed experimental behavior.

Fig. 4 shows the modeled time response of the gap voltage U_a and the inferred force F_{el} for one high frequency case with capacitive behavior (5000 Hz) on the right and one in the transition range between resistive and capacitive behavior (100 Hz) on the left. The model parameters are chosen as in Table 1. For the 100 Hz case, the gap voltage leads the excitation voltage by some degrees and the amplitude is approximately 60% of the excitation amplitude. Contrary, in the high frequency case the gap voltage is in phase with the excitation voltage and the amplitude transfers to more than 80%. Since the electroadhesive force is proportional to the square of the gap voltage, its frequency is twice the excitation frequency and the amplitude is significantly higher for the high frequency case.

Fig. 4 Modeled time response of the voltage U_a and the inferred electroadhesive force F_{el} for a sinusoidal excitation voltage with amplitude of $U_0 = 200$V at frequencies of 100Hz (left) and 5000 Hz (right), both at an external force of $F_N = 0.5$N

Fig. **5** shows the time responses for a square wave excitation for the frequencies of, again, 100 Hz on the left and 5000 Hz on the right. For each sudden change in excitation voltage, a maximum or minimum in the gap voltage follows. During the phases of constant excitation voltage, the gap voltage drops due to leakage through the resistors. This voltage drop is significant for the 100 Hz case, causing a very volatile time response of the inferred force. For the high frequency case, the gap voltage drop is much less significant and the resulting model prediction of the force is almost constant in time.
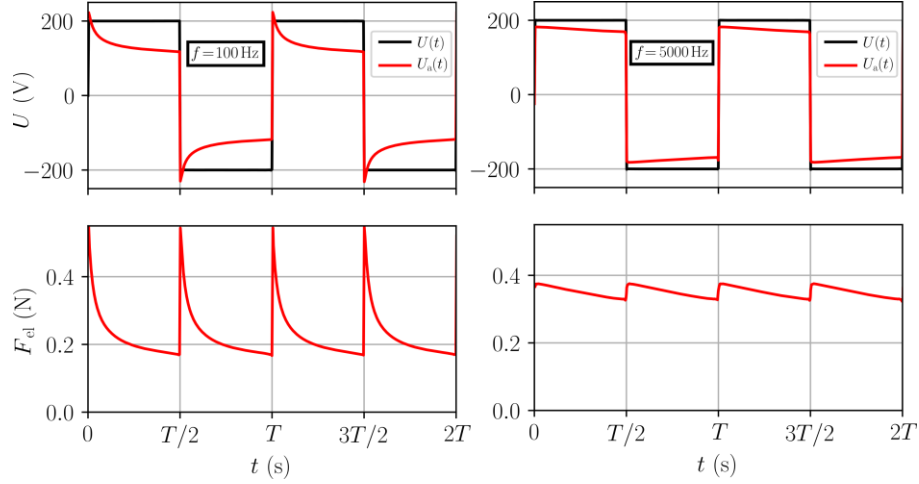
Fig. 5 Modeled time response of the voltage U_a and the inferred electroadhesive force F_{el} for a square wave excitation voltage with amplitude of $U_0 = 200V$ at frequencies of 100Hz (left) and 5000 Hz (right), both at an external force of $F_N = 0.5N$

5. CONCLUSIONS

To model the observed frequency dependence in the electroadhesive frictional contact of a finger pad with a touchscreen, an extension of the macroscopic model recently developed by the authors has been proposed. The impedance behavior observed in experiments, resistive for low frequencies and capacitive for high frequencies, was successfully modeled by three parallel circuits of resistor and capacitor in series, one for each electrical layer. The electromechanical parameters were chosen according to recent measurements and the model predictions of the inferred electroadhesive force were compared to a recent experimental study [6]. The model predictions agree qualitatively and quantitatively reasonably well with experimental results. The present model further shows that the significant scattering of the experimental data for different subjects may be due to the variability of crucial parameters such as the ridge contact area, the equivalent interfacial gap thickness and the electrical resistance of the interfacial gap. However, further validation with a more complete experimental data set is needed. Finally, the time response of the developed model to different wave forms and frequencies of the excitation voltage is presented and discussed.

REFERENCES

1. Bau, O., Poupyrev, I., Israr, A., Harrison, C., 2010, *Teslatouch: Electrovibration for Touch Surfaces*, UIST 2010 - 23rd ACM Symposium on User Interface Software and Technology, pp. 283-292.
2. Vardar, Y., Güçlü, B., Basdogan, C., 2017, *Effect of waveform on tactile perception by electrovibration displayed on touch screens*, IEEE Transactions on Haptics, 10, pp. 488-499.
3. Grimnes, S., 1983, *Electrovibration, cutaneous sensation of microampere current*, Acta Physiologica Scandinavica, 118, pp. 19-25.
4. Liu, X., Lu, Z., Lewis, R., Carré, M.J., Matcher, S.J., 2013, *Feasibility of using optical coherence tomography to study the influence of skin structure on finger friction*, Tribology International, 63, pp. 34-44.

5. van Kuilenburg, J.V., Masen, M.A., van der Heide, E., 2013, *A review of fingerpad contact mechanics and friction and how this affects tactile perception*, Proceedings of the Institution of Mechanical Engineers, Part J: Journal of Engineering Tribology, 229, pp. 243–258.

6. Meyer, D.J., Peshkin, M.A., Colgate, J.E., 2013, *Fingertip friction modulation due to electrostatic attraction,* 2013 World Haptics Conference (WHC), pp. 43-18.

7. Vezzoli, E., Amberg, M., Giraud, F., Lemaire-Semail, B., 2014, *Electrovibration Modeling Analysis,* Haptics: Neuroscience, Devices, Modeling, and Applications Lecture Notes in Computer Science, pp. 369–376.

8. Shultz, C.D., Peshkin, M.A., Colgate, J.E., 2015*, Surface haptics via electroadhesion: Expanding electrovibration with Johnsen and Rahbek*. 2015 IEEE World Haptics Conference (WHC), pp. 57-62.

9. Nakamura, T., Yamamoto, A., 2017, *Modeling and control of electroadhesion force in DC voltage*, ROBOMECH Journal, 4, 18.

10. Heß, M., Forsbach, F., 2020, *Macroscopic Modeling of Fingerpad Friction Under Electroadhesion: Possibilities and Limitations*, Frontiers in Mechanical Engineering, 6, 77.

11. Gao, J., Luedtke, W.D., Gourdon, D., Ruths, M., Israelachvili, J., Landman, U., 2004, *Frictional forces and amontons' law: From the molecular to the macroscopic* scale, Journal of Physical Chemistry B, 108, pp. 3410-3425.

12. Popov, V.L., Dimaki, A.V., 2017, *Friction in an adhesive tangential contact in the Coulomb-Dugdale approximation*, The Journal of Adhesion, 93(14), pp. 1131–1145.

13. Sahli, R., Pallares, G., Ducottet, C., Ben Ali, I.E., Al Akhrass, S., Guibert, M., Scheibert, J., 2018, *Evolution of real contact area under shear and the value of static friction of soft materials*, Proceedings of the National Academy of Sciences of the United States of America, 115, pp. 471-476.

14. Heß, M., Popov, V.L., 2019, *Voltage-induced friction with application to electrovibration*, Lubricants, 7(12), 102.

15. Shultz, C.D., Peshkin, M.A., Colgate, J.E., 2018, *On the electrical characterization of electroadhesive displays and the prominent interfacial gap impedance associated with sliding fingertips*. 2018 IEEE Haptics Symposium (HAPTICS), pp. 151-157.

16. Fruhstorfer, H., Abel, U., Garthe, C.-D., Knüttel, A., 2000, *Thickness of the stratum corneum of the volar fingertips*, Clinical Anatomy, 13, pp. 429–433.

17. Yamamoto, T., Yamamoto, Y., 1976, *Dielectric constant and resistivity of epidermal stratum corneum*, Medical & Biological Engineering, 14, pp. 494–500.

18. Choi, C., Ma, Y., Li, X., Ma, X., Hipwell, Mary, 2021, *Finger pad topography beyond fingerprints: understanding the heterogeneity effect of finger topography for human–machine interface modeling*, ACS Applied Materials & Interfaces, 13, pp. 3303–3310.

19. Dzidek, B.M., Adams, M.J., Andrews, J.W., Zhang, Z., Johnson, S.A., 2017, *Contact mechanics of the human finger pad under compressive loads*, Journal of The Royal Society Interface, 14, 20160935.

20. Vezzoli, E., Ben Messaoud, W., Nadal, C., Frédéric, G., Amberg, M., Lemaire-Semail, B., Bueno, M.A., 2015, *Coupling of ultrasonic vibration and electrovibration for tactile stimulation*, European Journal of Electrical Engineering, 17, pp. 377-395.